# Evaluation of polyelectrolyte complex-based scaffolds for mesenchymal stem cell therapy in cardiac ischemia treatment

Caroline Ceccaldi [a,b,*], Raya Bushkalova [a,b], Chiara Alfarano [b], Olivier Lairez [b], Denis Calise [b], Philippe Bourin [e], Celine Frugier [b], Charlotte Rouzaud-Laborde [b,d], Daniel Cussac [b,c], Angelo Parini [b,c,d], Brigitte Sallerin [b,c,d,1], Sophie Girod Fullana [a,1]

[a] Université de Toulouse, CIRIMAT, UPS-INPT-CNRS, Faculté de Pharmacie, F-31062 Toulouse, France
[b] INSERM, UMR 1048, F-31432 Toulouse, France
[c] Université de Toulouse, UPS, Faculté des Sciences Pharmaceutiques, F-31062 Toulouse, France
[d] CHU Toulouse, Service de Pharmacie Hospitalière, F-31432 Toulouse, France
[e] EFS, Laboratoire de thérapie cellulaire, F-31027 Toulouse, France

A B S T R A C T

Three-dimensional (3D) scaffolds hold great potential for stem cell-based therapies. Indeed, recent results have shown that biomimetic scaffolds may enhance cell survival and promote an increase in the concentration of therapeutic cells at the injury site. The aim of this work was to engineer an original polymeric scaffold based on the respective beneficial effects of alginate and chitosan. Formulations were made from various alginate/chitosan ratios to form opposite-charge polyelectrolyte complexes (PECs). After freeze-drying, the resultant matrices presented a highly interconnected porous microstructure and mechanical properties suitable for cell culture. In vitro evaluation demonstrated their compatibility with mesenchymal stell cell (MSC) proliferation and their ability to maintain paracrine activity. Finally, the in vivo performance of seeded 3D PEC scaffolds with a polymeric ratio of 40/60 was evaluated after an acute myocardial infarction provoked in a rat model. Evaluation of cardiac function showed a significant increase in the ejection fraction, improved neovascularization, attenuated fibrosis as well as less left ventricular dilatation as compared to an animal control group. These results provide evidence that 3D PEC scaffolds prepared from alginate and chitosan offer an efficient environment for 3D culturing of MSCs and represent an innovative solution for tissue engineering.

*Keywords:*
Alginate
Chitosan
Mesenchymal stem cells
Cell therapy
Myocardial infarction

## 1. Introduction

Regeneration of the myocardium is a slow process, limiting cardiac repair after ischemic injury. Therefore, myocardial infarction (MI) frequently leads to progressive cardiac damage and, finally, to heart failure [1]. Previous studies have shown that administration of autologous bone marrow mesenchymal stem cells (MSCs) prevents cardiac damage and improves ventricular function after ischemic insult [2,3]. Most of the beneficial effects of MSCs have been related to the secretion of a variety of paracrine factors [4–8]. Therefore, the possibility of concentrating MSCs within or in proximity of the damaged tissue is an obvious strategy to enhance the local concentration of secreted paracrine factors. However, most of the cells injected into the cardiac parenchyma (~85%) die within 3 days of administration [9–14]. This early cell death significantly decreases the efficacy of cell therapy. An alternative strategy to intraparenchymal cell injection is the use of tailored scaffolds providing a biomimetic and protective environment for MSCs [15,16]. This could improve MSC survival and, consequently, the enhance the beneficial effects related to the secretion of paracrine factors.

Alginates are widely used in regenerative medicine because of their gelling properties under conditions compatible with biological activities (37 °C, pH 7.4), their low toxicity after purification and their high biocompatibility related to their biomimetic structure. They are a family of naturally derived polymers extracted from marine brown algae. Alginates are unbranched binary copolymers consisting of 1,4-linked β-D-mannuronic (M) and α-L-guluronic (G) residues organized in regions of sequential G units (G-blocks), regions of sequential M units (M-blocks) and regions of atactically organized G and M units. The sol–gel transition properties of alginates are based on the formation of a stiff "egg-box" structure due to the selective binding of divalent cations to

* Corresponding author at: Laboratoire de Pharmacie Galénique. CIRIMAT - UMR 5085 UPS-INPT-CNRS - Institut Carnot. Equipe "Phosphates, Pharmacotechnie, Biomateriaux". Faculté des Sciences Pharmaceutiques 31062 Toulouse cedex 09. Tel.: (+33) 5 62 25 68 39. Fax: (+33) 5 62 25 68 39.
*E-mail address:* caroline.ceccaldi@inserm.fr (C. Ceccaldi).
[1] These authors contributed equally to this work.

http://dx.doi.org/10.1016/j.actbio.2013.10.027

G-blocks of two adjacent polymeric chains [17]. Alginate associations with cardiac precursors for myocardium substitute formation have been proven to have beneficial impact on supporting cell survival and proliferation [18,19], inducing neovascularization, and promoting the integration of the structure in a cardiac neoformation context [20–22]. However, the efficacy of alginate-based materials is limited by their physical properties [23], and these materials need to be improved to control the macroporosity in the resulting scaffolds and to enhance mechanical performance. In addition, with the goal to take advantage exclusively of the paracrine activity of implanted cells, the adhesion properties of alginate scaffolds should be emphasized to optimize cellretention and promote cell proliferation [15]. Strategies to improve alginate properties may entail chemical modifications leading to the generation of potentially toxic reactive intermediates. One alternative to chemical modifications is to combine alginate with a cationic biocompatible polymer to obtain polyelectolyte complexes with improved characteristics.

Chitosan is a cationic copolymer of β(1-4)-2-acetamido-2-deoxy-β-D-gucopyranose and 2-amino-2-deoxy-β-D-glucopyranose, obtained by deacetylation of naturally occurring chitin. It is biocompatible and biodegradable, and is able to promote wound healing [24] and cell adhesion alone [25], or associated with other polymers [26]. Although its ability to form porous polyelectrolyte complexes (PECs) when associated with alginates has already been described [27], the use of alginate- and chitosan-based scaffolds incorporating MSCs for the treatment of heart failure has never been proposed.

In the present study, we designed three-dimensional (3D) PEC scaffolds, and evaluated their physical and biological characteristics and their impact on MSC retention, survival and function. In addition, we studied the effects of MSCs seeded on 3D PEC scaffolds in a rat model of acute MI.

## 2. Materials and methods

### *2.1. Design of 3D PEC scaffolds and 2D PEC film-coated wells 3D PEC scaffolds were prepared under aseptic conditions*

Alginate (medium-viscosity alginate, Sigma) dispersion: solutions of 1.5% (w/w) alginate were prepared in iso-osmotic saline solution for 30–120 min at 1200 rpm (Heidolph RZR-2041, Germany).

Chitosan dispersion: solutions of chitosan (medium MW, Sigma) were prepared in 0.25 M acid acetic iso-osmotic solution (150 mM NaCl) for 30 min at 1800–2000 rpm (Heidolph RZR-2041, Germany).

Alginate and chitosan solutions were mixed to obtain polyelectrolyte systems containing different weight ratios of alginate to chitosan (single polysaccharide, and alginate/chitosan weight ratios of 60/40, 50/50 and 40/60).

3D PEC scaffolds, 5 mm diameter × 2.5 mm thick, were generated by a freeze-drying technique described by Shapiro and Cohen [28]. Briefly, aliquots (100 μl) of polyelectrolyte solutions were placed in a 96-well plate, frozen overnight at −20 °C and lyophilized. Constructs were cross-linked in an iso-osmotic buffer containing calcium ions (150 mM NaCl, $CaCl_2$, 0.1 M, 12.5 mM Hepes, pH 7.4) during 60 min. Pure chitosan scaffolds (with a alginate/chitosan ratio of 0/100) were gellified with 1 M NaOH. Scaffolds were washed twice (10 min in Hepes buffer) and lyophilized again.

2D PEC films coating the wells of an 8-well microscope slide were obtained by adding 0.07 g of polyelectrolyte solution to each well. 2D PEC films were dried overnight at 37 °C and cross-linked with an iso-osmotic buffer containing calcium ions (150 mM NaCl, $CaCl_2$, 0.1 M, 12.5 mM Hepes, pH 7.4) for 60 min. Pure chitosan 2D films were gellified with 1 M NaOH. 2D films were washed twice (10 min in Hepes buffer, pH 7.4) and dried again at 37 °C.

3D PEC scaffolds and 2D PEC film-coated wells scaffolds were sterilized by exposure to UV light.

### *2.2. Scanning electron microscopy (SEM)*

SEM analysis of the surface and cross-section of dried 3D PEC scaffolds was performed with a Leo 435 VP scanning electron microscope. The scaffold samples were mounted on an aluminum sample mount and sputter-coated with silver. The specimens were observed at a 10 kV accelerating voltage. Pore diameter was determined by measuring the diameter of 10 pores on surface and cross-section images ($n$ = 10).

### *2.3. Mechanical properties*

The differential elastic moduli and the mechanical behavior of the scaffolds were measured by three successive uniaxial compressive assays (TA-XT2 texture analyzer, Stable Microsystems, UK). The apparatus consisted of a mobile probe (314.16 $mm^2$) moving vertically up and down at a constant and predefined velocity (0.5 mm $s^{-1}$). The force exerted by the probe on the scaffolds was recorded as a function of the displacement. The force was converted to stress by reporting the force to the surface of force application, and displacement was converted to a strain percentage in comparison with the initial shape. Differential elastic moduli were calculated from the stress–strain curves at 50% of strain and represent the relative stiffness of the scaffold at 50% strain. The differential elastic modulus was expressed as follows from at least three independent observations: $E_{50\%} = [(F_{50\%}/S)/\text{Strain}] \times 1000$ kPa, where $F_{50\%}$ is the force registered at 50% strain (N) and S is the surface of the specimen ($mm^2$).

### *2.4. Isolation and culture of human MSCs for in vitro experiments*

Human MSCs were isolated from PBS-washed filters used during bone marrow (BM) graft processing for allogenic BM transplantation. Cells were cultured at a density of $5 \times 10^4$ cells $cm^{-2}$ in α-Minimum Essential Medium (α-MEM, Invitrogen, San Diego, CA, USA) supplemented with 10% fetal calf serum (Hyclone, Logan, UT, USA) and ciprofloxacin (10 mg $ml^{-1}$; Bayer Schering Pharma, Germany). After 72 h at 37 °C in 5%$CO_2$, non-adherent cells were removed and the medium was changed. Cultures were fed every 3–4 days. MSCs were able to differentiate into osteoblasts, chondroblasts and adipocytes and were $CD90^+$ (99.1 ± 1.2%), $CD45^-$ (3.6 ± 1.8%), $CD34^-$ (1.9 ± 2.3%), $CD73^+$ (100 ± 0%), $CD31^-$ (1.2 ± 0.8%), $CD105^+$ (99 ± 0.7%), $CD29^+$ (99.9 ± 0.05%) and $CD13^+$ (99.9 ± 0.2%), data not shown. MSCs were used between the third and sixth passages.

### *2.5. Isolation and culture of rat MSCs for in vivo experiments*

MSCs were obtained from BM of Lewis male rats (Harlan, France) weighing 180–200 g. Anesthesia was performed by intraperitoneal injection of pentobarbital (0.1 ml/100 g). BM was flushed from rat femur with α-MEM (Gibco, France) supplemented with 10% fetal bovine serum and 1% penicillin/streptomycin (Invitrogen, France) and centrifuged (400*g*, 5 min). Then, cells were plated in culture flasks (100,000 cells $cm^{-2}$). After 3 days, non-adherent cells were removed by changing medium, and MSCs were recovered by their capacity to adhere to plastic culture dishes. MSCs were then routinely labeled and cultured for the experiments.

### 2.6. MSC seeding and cultivation

For in vitro studies, the cells were seeded onto the scaffolds by dropping 10 μl of cell suspension containing 20,000 cells on top of the dried scaffolds. After a short centrifugation (400*g*, 1 min), seeded scaffolds were hydrated by adjusting the volume of culture medium. Constructs were cultured at 37 °C in 5%$CO_2$. The medium was changed every 3–4 days.

### 2.7. Adhesion measurement with human MSCs

#### 2.7.1. Immunocytochemistry of cytoskeleton proteins

3D PEC scaffolds seeded with hMSCs were fixed with paraformaldehyde and incubated with Alexafluor 488-phalloidin (1 h, 1:40, Invitrogen) and mouse anti-human vinculin (1 h, 1:100, Sigma–Aldrich) for detection of actin and focal adhesion, respectively. Antibody detection was performed by using an Alexafluor 568 secondary antibody (1:200, 30 min; Invitrogen, CA). For nucleus detection, sections were incubated with DAPI (0.08 μg $ml^{-1}$, 20 min; Invitrogen, CA).

#### 2.7.2. Confocal imaging

MSCs were cultured on 3D PEC scaffolds for 3 days. After immunostaining of cytoskeleton proteins, 3D PEC scaffolds were photographed using an Axio Observer Z1 microscope (Zeiss, Germany) with a ×63 objective.

#### 2.7.3. Evaluation of cell spreading

MSCs were cultured on 2D PEC films for 3 days. After immunostaining of cytoskeleton proteins, films were analyzed using an Axio Observer Z1 microscope with a ×10 objective. Mean cell area was determined on randomly selected images (6–7) of 2D PEC films for each alginate/chitosan proportion ($n$ = 50 cells for each group).

### 2.8. Quantification of MSC metabolism activity

Cell metabolism activity was quantified by alamarBlue® assay (Molecular Probes, Invitrogen, France). 3D PEC scaffolds were transferred to new wells and incubated with 1 ml of minimal essential medium (Gibco, France) supplemented with 10% of alamarBlue® reagent for 1–4 h as specified by the manufacturer. Aliquots of 100 μl were transferred to a 96-well plate and the fluorescence was measured at an excitation wavelength of 540 nm and an emission wavelength of 620 nm using a plate reader (Infinite®200Pro, Tecan Group).

### 2.9. Growth factor release

After cell seeding, 3D PEC scaffolds were hydrated by adjusting the volume of culture medium and cultured at 37 °C in 5% $CO_2$ for 24 h under sterile conditions. The amount of HGF, FGF-2 and VEGF released into the medium was quantified in the supernatant by xMAP technologies (Luminex 100™ system, Luminexcorp) with anti-human HGF, FGF-2 and VEGF antibodies (Ozyme, France).

### 2.10. In vivo implantation of polyelectrolyte scaffolds

Animals were handled in accordance with the European Animal Care Guidelines. 3D PEC scaffolds were implanted in adult female rats (200–250 g) by left thoracotomy via the fourth *intercostal space* under general anaesthesia (isoflurane, 2.5%) and mechanical ventilation. After a pericardectomy, left anterior descending (LAD) artery was definitively ligated using a 7–0 prolene suture. 3D PEC scaffolds (alginate/chitosan weight ratio of 40/60) with ($5 \times 10^5$ cells, $n$ = 6) or without ($n$ = 4) rat MSCs were implanted just after MI. Scaffolds were placed on the surface of the left ventricle and fixed by one suture using a 7-0 prolene suture. The control group was subjected to the same surgical procedure without scaffold implantation ($n$ = 3) and sham-operated animals were subjected to the same surgical procedure without LAD artery ligation and scaffold implantation ($n$ = 4).

### 2.11. Blood analysis

Hematocrit measurement was performed on blood collected by retro-orbital bleeding on anesthetized animals using heparinized tubes. Hematocrits were evaluated by a standard microhematocrit method. Leukocyte differential count was performed on total blood collected from the abdominal aorta (MICROS-60, ABX-Diagnostics, France).

### 2.12. Echography

Left ventricular (LV) function was assessed in anesthetized animals with two-dimensional echocardiography with a General Electric Vivid 7® (GE Medical System, USA) equipped with a 13 MHz linear probe. Anesthesia was induced with isoflurane and the rats received continuous inhaled anesthetic (2%) for the duration of the imaging session. The animals were placed in the supine or lateral position on a warming pad. Numeric images of the heart were obtained in both parasternal long-axis and short-axis views. 2D end-diastolic and end-systolic long-axis views of the LV were standardized as follows: inclusion of the apex, the posterior papillary muscle, the mitral valve and the aortic root. 2D echocardiographic measurements were performed with the cine-loop feature to retrospectively catch true end-diastolic and end-systolic phases, defined as the phases in which the largest and the smallest LV cavity size was obtained, respectively. End-diastolic and end-systolic areas (A) were obtained by hand tracings of the LV endocardial contours, according to the American Society of Echocardiography leading-edge method. On these frames, end-diastolic and end-systolic lengths (L) of the LV were obtained by tracing a line connecting the more distal part of the apex and the center of a line connecting the mitral annular hinge points. End-diastolic and end-systolic volumes (LVEDVs and LVESVs, respectively) were then calculated by means of the single-plane area–length method (volume = $8 \times A^2/3 \times \pi \times L$). LV ejection fraction (LVEF,%) was calculated as [(LVEDV − LVESV)/LVEDV] × 100. All measurements were averaged over three consecutive cardiac cycles and analyzed by a single observer who was blinded to the treatment status of the animals.

### 2.13. Histological examinations

Heart tissue specimens were fixed in Carnoy's solution and embedded in paraffin.

For light microscopic investigations, paraffin sections (4 μm) were stained with Sirius red (Sigma Aldrich, France). Three different histological preparations obtained from each animal were scanned (NanoZoomer Digital Pathology) and semiquantified microscopically using MorphoExpert software. The percentage of fibrosis was estimated from the Sirius red-stained surface compared to the total heart tissue area without PEC scaffold. Scar and septum thickness were measured at three different random sites and relative scar thickness was calculated as the mean scar thickness/septum thickness.

For immunofluorescence experiments, paraffin sections (4 μm) were rehydrated and incubated with mouse monoclonal anti-α-SMA (1:1000, clone 1A4, Sigma, USA) for 2 h. Antibody revelation was performed by using an Alexafluor 568 secondary antibody (1:2000, 45 min; Invitrogen, CA). For nucleus detection, sections were incubated with DAPI (0.08 μg $ml^{-1}$, 20 min; Invitrogen, CA).

The slides were photographed using an Axio Observer.Z1 microscope with a ×10 objective. Blood vessel density (number $mm^{-2}$) was determined by combining counting of α-SMA-positive structures and morphological analysis. Four randomly selected images of the ischemic area and border zone stained by α-SMA fluorescent antibody were quantified for each animal.

### 2.14. Statistical analysis

Results are expressed as mean ± SEM. Statistical comparison of the data was performed using the *t*-test for comparison between two groups or one-way ANOVA and post hoc Bonferroni's test for comparison of more than two groups. A value of $P < 0.05$ was considered significant.

## 3. Results

### 3.1. Characterization of 3D PEC scaffold complexes

#### 3.1.1. Morphology and porosity of polymeric scaffolds

Three different scaffolds with a constant alginate concentration (1.5% w/w) and containing 60/40, 50/50 and 40/60 alginate/chitosan ratios (w/w) were synthesized as described in the Materials and methods section. Control scaffolds composed of pure alginate (1.5% w/w, defined as 100/0 alginate/chitosan ratio) or with pure chitosan (1.5% w/w, defined as 0/100 alginate/chitosan ratio) were synthesized according to the same procedure. Fig. 1 shows SEM images of the surface (Fig. 1A–E) and the cross-section (Fig. 1F–J) of 100/0 (Fig. 1A and F), 60/40 (Fig. 1B and G), 50/50 (Fig. 1C and H), 40/60 (Fig. 1D and I) and 0/100 (Fig. 1E and J) of the 3D PEC scaffolds.

All 3D PEC scaffolds displayed an interconnected porosity in their surface and cross-section. On the surface, the pore density appeared to increase with increasing chitosan proportion. In the cross-section, scaffolds composed of combined alginate and chitosan polymers displayed approximately the same pore density as pure alginate scaffolds. In comparison, pure chitosan scaffolds exhibited a higher pore density.

Quantitative determination of pore size showed that the mean pore diameter of the scaffolds was between 50 and 200 μm on the surface (Fig. 1K) and between 100 and 200 μm in the cross-section (Fig. 1L). In particular, the largest pore diameters were observed when scaffolds were synthesized from 60/40 (surface 174 ± 19 μm; cross-section 190.7 ± 20.7 μm) and 40/60 (surface 143.4 ± 14.4 μm; cross-section 200.7 ± 22.8 μm) mixtures.

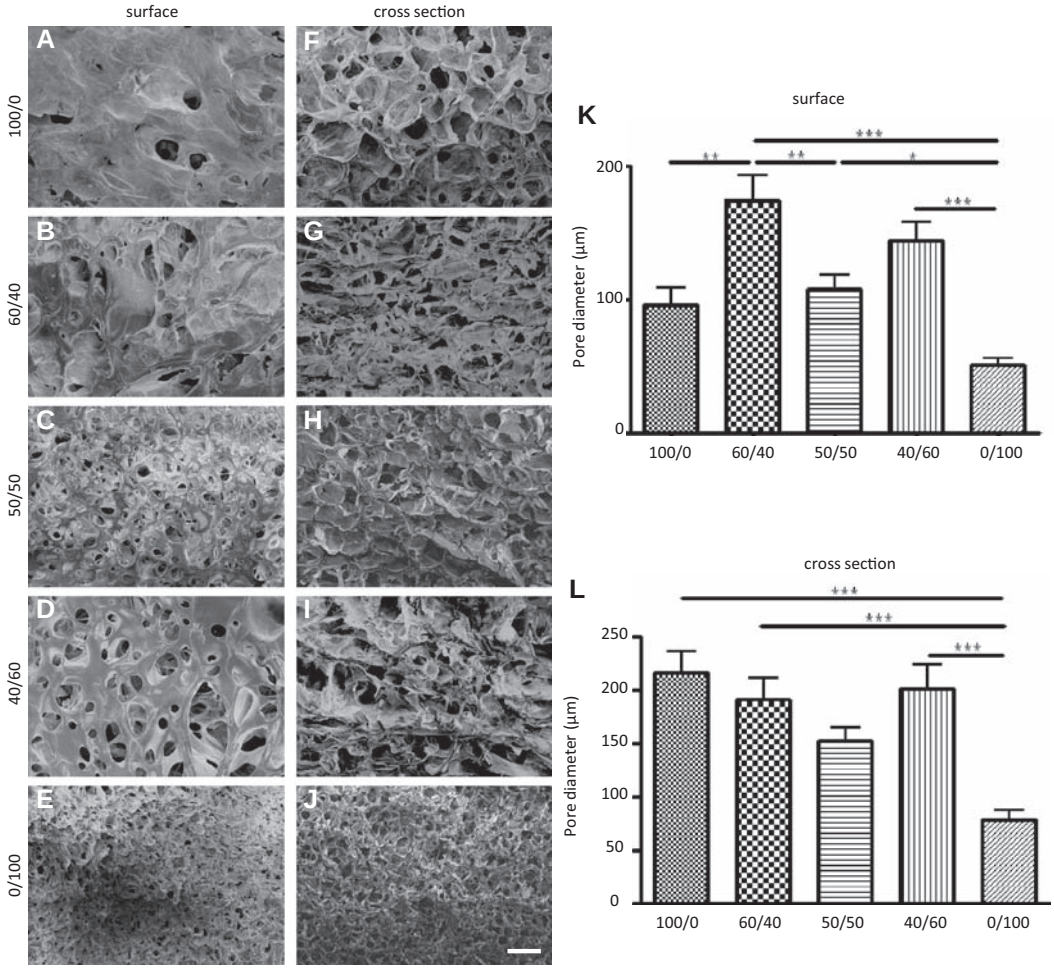


**Fig. 1.** Morphology and porosity of 3D PEC scaffolds with various weight alginate/chitosan weight ratios. Different PEC scaffold formulations were synthesized with various alginate/chitosan ratios. Scaffold compositions are: 100/0: 1.5% alginate; 60/40: 1.5% alginate + 1% chitosan; 50/50: 1.5% alginate + 1.5% chitosan; 60/40: 1.5% alginate + 2.25% chitosan; 0/100: 1.5% chitosan. Representative SEM images of scaffold surfaces (A–E) and cross-section (F–J) of 3D PEC scaffolds. Scale bar corresponds to 200 μm. Determination of surface (K) and cross-section (L) porosity of 3D PEC scaffolds with various alginate/chitosan weight ratios (100/0, 60/40, 50/50, 40/60, 0/100). Measurements were obtained from SEM images. $^{*}P \leqslant 0.05$, $^{**}P \leqslant 0.01$, $^{***}P \leqslant 0.001$ and based on ANOVA analysis.

*3.1.2. Mechanical properties of 3D PEC scaffolds*

In order to evaluate the plasticity/viscosity of scaffolds, which is significant to their in vivo interaction with contractile myocardium, the mechanical behavior of 3D PEC scaffolds was assessed by compressive tests after rehydratation in α-MEM culture medium. Stress–strain curves recorded during the compression were not linear for all formulations (Fig. 2A), indicating a non-Hookean behavior of these polymeric scaffolds. The differential elastic modulus at 50% strain was determined after three successive compressions with an interval of 30 min to determine if the mechanical behavior changed in a time-dependent manner (Fig. 2 B). 3D PEC scaffolds presented higher differential elastic moduli (60/40: 17.1 ± 1.6 kPa; 50/50: 34.5 ± 5.4 kPa; 40/60: 31.0 ± 1.4 kPa) than pure alginate scaffolds (100/0: 1.6 ± 0.07 kPa) or pure chitosan scaffolds (0/100: 4.0 ± 0.12 kPa). The differential elastic moduli of the PEC formulations 60/40, 50/50 and 40/60 varied in a time-dependent manner according to the plastic and/or viscous properties of these scaffolds. In contrast, pure alginate and pure chitosan scaffolds maintained their initial properties. At the end of the first compression, PEC scaffolds did not recover instantaneously their initial physical shape. Consequently, 30 min later, when compressed for the second time, the scaffolds, now more compact, presented a higher differential elastic modulus. Unlike the PEC scaffolds, the pure alginate and pure chitosan scaffolds did recover their initial mechanical properties/shape after compression. Mechanical properties were significantly improved when alginate and chitosan were associated.

*3.2. In vitro evaluation of 3D PEC scaffolds*

Human MSC compatibility was studied through the evaluation of their metabolic activity, attachment and secretory properties. Scaffold seeding was performed by the centrifugation procedure described by Dar et al. [18].

*3.2.1. Cell attachment on PEC scaffolds*

MSC adhesion in the different alginate/chitosan formulations was followed by immunostaining with antibodies against F-actin (green), a cytoskeleton microfilament, and vinculin (red), a focal adhesion protein, 3 days after seeding (Fig. 3).

MSCs cultivated in the 3D PEC scaffolds with a 60/40 and 50/50 ratio maintained their spherical shape, and their morphology revealed a non-organized cytoskeleton. In addition, no focal adhesion points between cells/scaffolds were found. For an alginate/chitosan ratio of 40/60, we observed an organized cytoskeleton with many focal adhesion points, as shown by the staining for F-actin and vinculin, respectively (Fig. 3A). A quantitative description of cell–scaffold interaction was evaluated by measuring the mean cell area 3 days after seeding on 2D PEC films (Fig. 3B). Results revealed the greatest cell surface when MSCs were cultured on pure chitosan 2D films (1268 ± 300 μm$^2$ for 0/100 polymer ratio) as compared to pure alginate 2D films (317 ± 26 μm$^2$ for 100/0 polymer ratio). 2D PEC films presented an intermediate cell spreading (60/40: 505.5 ± 150 μm$^2$; 50/50: 366.5 ± 33; μm$^2$ 40/60: 569.4 ± 95 μm$^2$).

*3.2.2. Metabolic activity of MSCs cultured on 3D PEC scaffolds*

We investigated whether the alginate/chitosan ratio could affect cell retention/metabolic activity after seeding. To this end, 20 000 MSCs were seeded by centrifugation on each type of 3D PEC scaffold and metabolic activity was measured after 3 and 14 days of culture by Alamar Blue assay. Fig. 4 shows the relative fluorescence intensity of cells seeded on scaffolds. The results were normalized to the fluorescence intensity measured for 20 000 MSCs (the initial metabolic activity at the moment of seeding). Interestingly, 3 days after seeding, the relative fluorescent intensity was statistically higher in pure chitosan scaffolds than in other scaffold formulations ($P < 0.001$). Fourteen days after seeding, in all scaffolds, the relative fluorescence intensity reached values close to that observed in pure chitosan, suggesting that all the 3D PEC

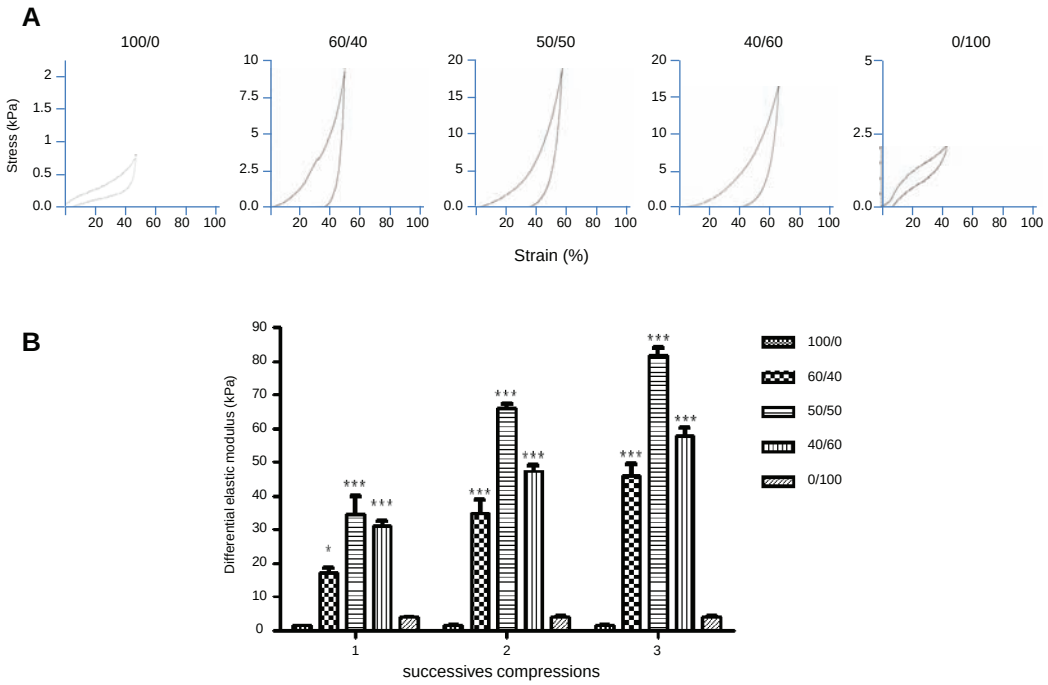


**Fig. 2.** Mechanical properties of 3D PEC scaffolds. Determination of the differential elastic modulus of scaffolds with various alginate/chitosan weight ratios (100/0, 60/40, 50/50, 40/60, 0/100) by measurement under three successive compressive strains (1, 2 and 3) at 30 min intervals. For statistical analysis, values are compared to alginate scaffold (with 100/0 alginate/chitosan weight ratio); $^{*}P \leqslant 0.05$, $^{***}P \leqslant 0.001$ and based on ANOVA analysis.

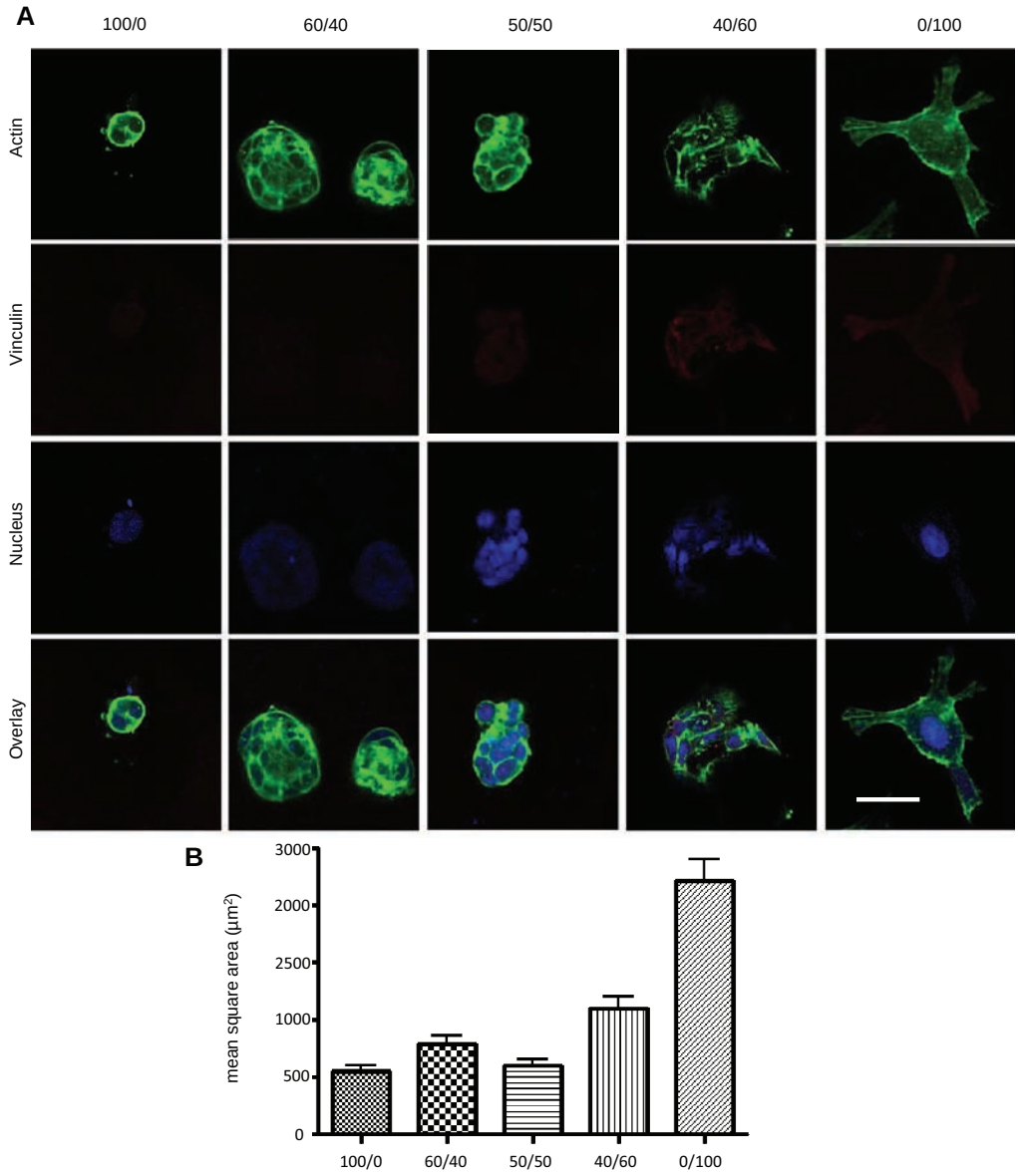


**Fig. 3.** Cell adhesion on PEC scaffolds. Immunostaining of actin (green), vinculin (red) and nuclei (blue) of human MSCs cultured on 3D PEC scaffolds on day 3 post-seeding. Scale bar corresponds to 50 μm (A). Human MSCs spreading on 2D PEC films of each formulation, expressed as mean cell area per single cell (B); no statistically difference was shown.

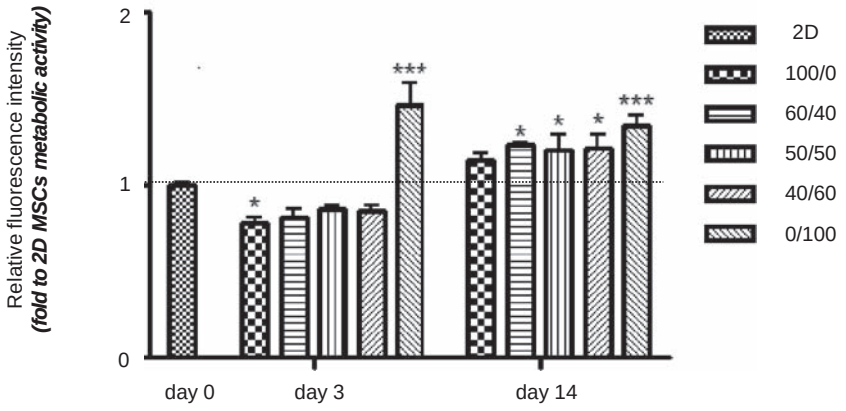


**Fig. 4.** MSC metabolic activity on 3D PEC scaffolds. Alamar Blue assays performed 3 and 14 days after cell seeding. The reference value was the fluorescence measured for 2D MSCs (20 000 cells, number of seeded cells) and is presented as 1 (dotted line) in the Fig. Results are fold metabolic activity of 20 000 MSCs. $^{**}P \leqslant 0.01$, $^{***}P \leqslant 0.001$, based on ANOVA analysis.

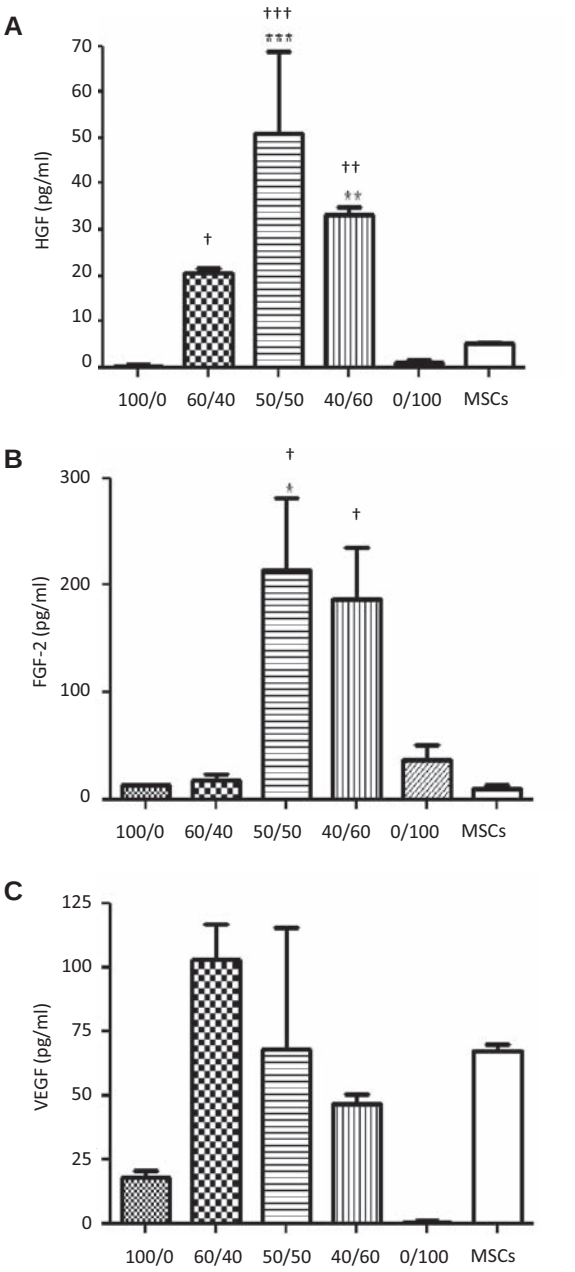


**Fig. 5.** Paracrine activity of seeded human MSCs. Quantification of HGF (A), FGF-2 (B) and VEGF (C) released in the supernatant by human MSCs cultured in 3D PEC scaffolds. Quantification was performed 24 h after seeding. ∗ denotes a significant difference compared to classical 2D culture of human MSCs on tissue culture plate ($^{**}P \leqslant 0.01$, $^{***}P \leqslant 0.001$, based on ANOVA analysis), and † denote a significant difference compared with human MSCs cultured on 100/0 3D alginate scaffolds ($^{\dagger}P \leqslant 0.05$, $^{\dagger\dagger}P \leqslant 0.01$, $^{\dagger\dagger\dagger}P \leqslant 0.001$, based on ANOVA analysis).

scaffolds stimulate cell proliferation and/or metabolic activity. These results show that the 3D PEC scaffold composition can affect cell retention and/or metabolic activity in these scaffolds.

### 3.2.3. Paracrine activity of seeded MSCs

Paracrine factors secreted by MSCs play a major role in the beneficial effects of cell therapy. Therefore, the functionality of MSCs was investigated by quantification of HGF, FGF-2 and of the angiogenic factor VEGF released in the supernatant of MSCs cultured in 3D PEC scaffolds. Analyses were performed 24 h after cell seeding and the results were compared to the secretion levels obtained in classical 2D culture plates of MSCs.

**Table 1**
Evaluation of 3D PEC scaffold biocompatibility. White blood cell differential count, hematocrit levels, lymphocytes, monocytes and granulocytes blood concentrations of implanted rats at the baseline, 7 and 33 days after surgical procedure.

| Day | Sham | MI | MI + Patch | MI + patch + MSCs | *P*-value |
|---|---|---|---|---|---|
| *White blood cells ($10^3$ mm$^{-3}$)* | | | | | |
| 0 | 9.45 ± 1.4 | 8 ± 3 | 10.3 ± 1.8 | 9.8 ± 4.2 | |
| 7 | 13.8 ± 2.8 | 10.3 ± 4.4 | 11.4 ± 3.6 | 10.8 ± 4.2 | $p > 0.05$ |
| 33 | 6.2 ± 0.6 | 9.5 ± 0.2 | 7 ± 1.1 | 6.7 ± 1.2 | $p > 0.05$ |
| *Hematocrit (%)* | | | | | |
| 0 | 45.2 ± 1 | 42.6 ± 0.1 | 43.7 ± 2.7 | 42.3 ± 2.8 | |
| 7 | 38.1 ± 1.5 | 37.3 ± 2.8 | 38.8 ± 1.6 | 40.3 ± 4.4 | $p > 0.05$ |
| 33 | 44.6 ± 0.6 | 42.8 ± 1.5 | 40.4 ± 3.3 | 42.0 ± 3.6 | $p > 0.05$ |
| *Lymphocytes ($10^3$ mm$^{-3}$)* | | | | | |
| 0 | 8.1 ± 0.6 | 7.0 ± 2.7 | 8.6 ± 1.4 | 8.4 ± 2.3 | |
| 7 | 10.8 ± 2.3 | 8.3 ± 3.0 | 7.7 ± 1 | 7.5 ± 1.5 | $p > 0.05$ |
| 33 | 7.3 ± 2.7 | 5.5 ± 0.8 | 5.5 ± 0.8 | 5.5 ± 1.1 | $p > 0.05$ |
| *Monocytes ($10^3$ mm$^{-3}$)* | | | | | |
| 0 | 0.8 ± 0.14 | 0.47 ± 0.21 | 0.80 ± 0.26 | 0.78 ± 0.35 | |
| 7 | 2.2 ± 0.49 | 1.13 ± 0.90 | 1.60 ± 1.00 | 1.44 ± 1.15 | $p > 0.05$ |
| 33 | 0.83 ± 0.53 | 0.53 ± 0.06 | 0.63 ± 0.15 | 0.54 ± 0.15 | $p > 0.05$ |
| *Granulocytes ($10^3$ mm$^{-3}$)* | | | | | |
| 0 | 0.7 ± 0.1 | 0.53 ± 0.21 | 0.98 ± 0.42 | 1.08 ± 0.51 | |
| 7 | 1.50 ± 0.1 | 0.90 ± 0.60 | 2.18 ± 1.65 | 2.02 ± 2.13 | $p > 0.05$ |
| 33 | 1 ± 0.53 | 0.70 ± 0.10 | 0.85 ± 0.25 | 0.66 ± 0.21 | $p > 0.05$ |

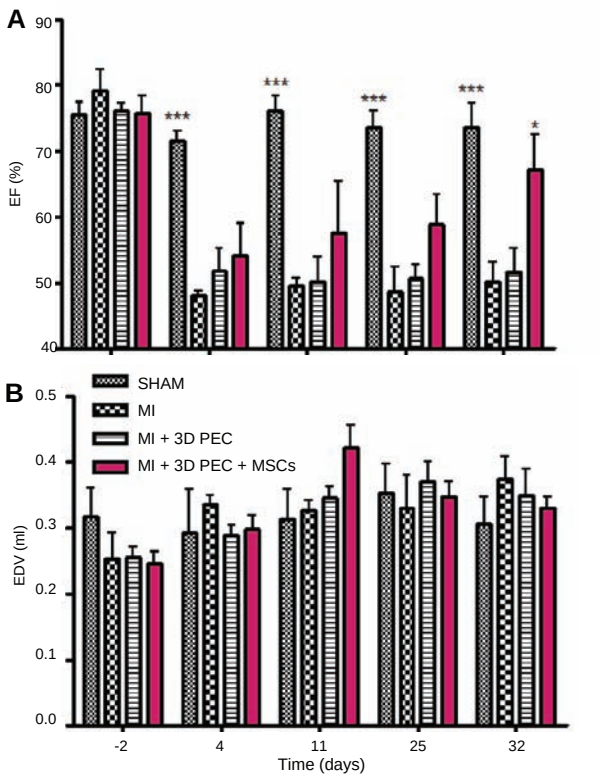


**Fig. 6.** Effect of 3D PEC scaffold implantation on cardiac function. Left ventricular ejection fraction (A) and left ventricular end-diastolic volume (B), assessed by echocardiography at the baseline (2 days before surgical procedure) and 4, 11, 25 and 32 days after surgical procedure. $^{*}P \leqslant 0.05$, $^{***}P \leqslant 0.001$ vs. MI, based on ANOVA analysis.

As shown in Fig. 5, we found that secretion of HGF (Fig. 5A), FGF-2 (Fig. 5B) and VEGF (Fig. 5C) by MSCs differed according to the culture conditions and the alginate/chitosan ratios. HGF and FGF-2 secretion in the extracellular medium was higher for alginate/chitosan ratios of 50/50 and 40/60 as compared to classical 2D culture. In contrast, VEGF secretion at these alginate/chitosan ratios was similar to that observed in MSC 2D culture. These results


**Fig. 7.** Macroscopic view of explanted 3D PEC scaffolds 33 days post-implantation. Scaffold covering the necrotic zone 33 days after the graft. Scale bar corresponds to 5 mm.

show that association of alginate and chitosan, in particular at 50/50 and 40/60 ratios, promotes, or at least maintains, the paracrine activities of MSCs.

### 3.3. In vivo evaluation of 3D PEC scaffolds

In vitro experiments showed that alginate/chitosan ratios of 50/50 and 40/60 were the most appropriate in term of microstructure, mechanical resistance and stimulation of MSC paracrine activity. In addition, an alginate/chitosan ratio of 40/60 appeared to promote cell adhesion and cytoskeleton organization. Therefore, we selected this formulation for the in vivo experiments.

#### 3.3.1. Cardiac implantation of 3D PEC scaffolds

The in vivo effects of 3D PEC scaffolds with an alginate/chitosan ratio 40/60 ratio were studied in a rat model of MI. MI was achieved by a definitive ligature of the left anterior descending artery. 3D PEC scaffolds were then fixed to the myocardium by a single suture onto the injured site. Rats were randomly distributed into four groups: (1) sham-operated animals (SHAM, $n = 4$), subjected to a thoracotomy and pericardectomy; (2) myocardial infarcted group (MI, $n = 3$), subjected to MI; (3) 3D PEC scaffold implanted group (MI + 3D PEC, $n = 4$), subjected to MI and implantation with an a cellular scaffold; and (4) group implanted with 3D PEC scaffolds seeded with MSCs (MI + 3D PEC + MSCs, $n = 6$), subjected to MI and implantation with a 3D PEC scaffolds seeded with rat bone marrow MSCs.

The in vivo compatibility of the 3D PEC scaffolds (seeded or not) was studied after implantation in a cardiac ischemic model. Hematocrit was analyzed and white blood cells were numbered at baseline and at 7 and 33 days after implantation in each different group. No significant differences were observed for these parameters between the control group, the MI group and the acellular scaffold- or MSC-seeded 3D PEC scaffold-implanted groups (Table 1).

#### 3.3.2. Cardiac function

Cardiac function was determined by echocardiography at baseline, 4, 11, 25 and 32 days after surgical procedure. The time course summary of echocardiography data is shown in Fig. 6. After MI (4 days after the beginning of the protocol), the ejection fraction decreased significantly (Fig. 6A, $P < 0.01$). The ejection fraction remained less than 50% for the group with MI and MI with acellular 3D PEC scaffolds during the time course of the protocol: 32 days. In contrast, the ejection fraction of the group with 3D PEC scaffolds seeded with MSCs (MI + 3D PEC + MSCs) showed an improvement compared to the control group (MI). Echocardiography performed at 32 days post-treatment demonstrated an improvement in LV function ($P < 0.05$). Statistically, the end-diastolic volume remained the same during the time course of the protocol (Fig. 6B).

#### 3.3.3. Macroscopic and microscopic observations of explants

Post-mortem analyses after 33 days post-implantation revealed that no adherences were observed in the environment of implanted 3D PEC scaffolds and in the thoracic wall. 3D PEC scaffolds were found still attached to the left ventricle, covering the ischemic area (Fig. 7).

Red Sirius staining of rat hearts (MI group, Fig. 8B–D) showed that rats with MI presented a decrease in the size of left ventricular wall associated with an intense fibrotic response compared to controls (Fig. 8A). This was confirmed by quantification of scar thickness (Fig. 8E) and fibrosis (Fig. 8F) in each group. A weak decrease in the fibrosis percentage was observed in rats implanted with acellular 3D PEC scaffolds as compared to rats without implanted scaffolds (Fig. 8F, $P > 0.05$). This tendency was more

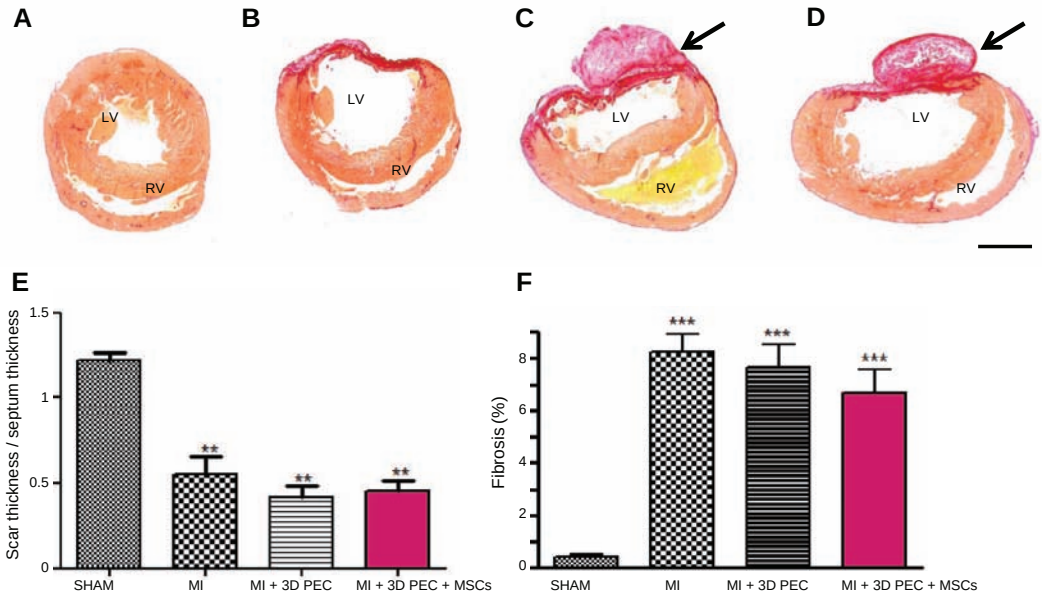


**Fig. 8.** Effect of 3D PEC scaffold implantation on myocardial fibrosis. Photomicrographs of myocardial sections stained with Sirius red of sham (A), infarcted rats without PEC scaffolds (B), implanted rats with PEC scaffolds without (C) and with MSCs (D). LV, left ventricles; RV, right ventricles; arrows indicate 3D PEC scaffolds grafted on the left ventricles. Scale bar corresponds to 2.5 mm. Quantitative analysis of (E) the scar thickness and (F) the fibrotic area in these three different groups. $^{**}P \leqslant 0.01$, $^{***}P \leqslant 0.001$, based on ANOVA analysis.

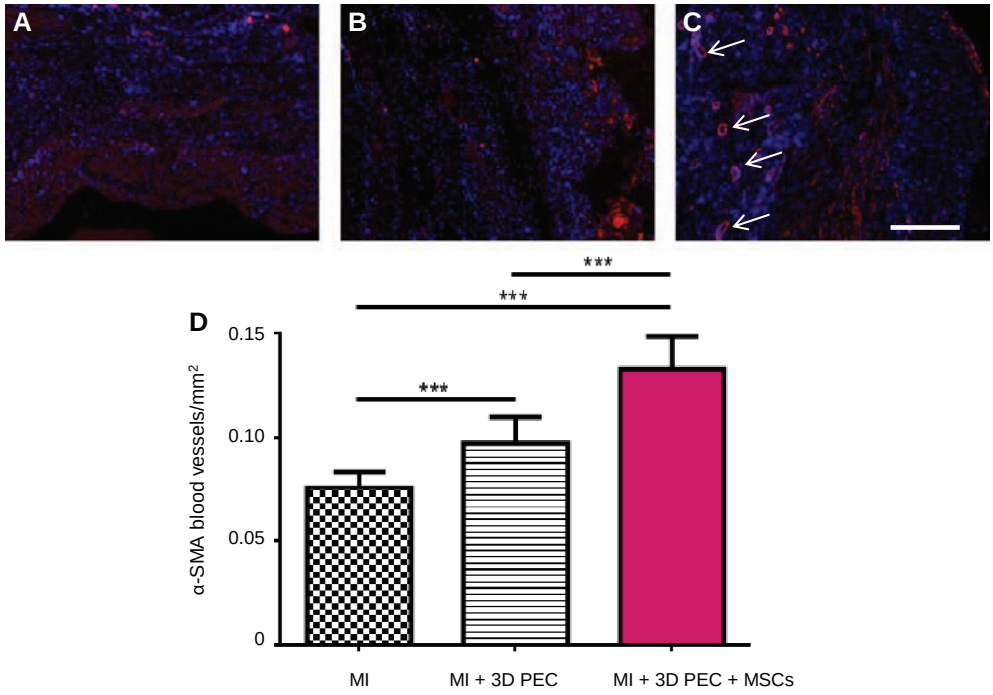


**Fig. 9.** Effect of 3D PEC scaffold implantation on neovascularization. Photomicrographs of myocardial sections immunostained with anti-α-SMA (red) in infarcted rats (A), PEC scaffold-implanted rats without (B) and with MSCs (C). Arrows in (C) show α-SMA-stained blood vessels. Scale bar corresponds to 200 μm. (D) Quantitative analysis of the blood vessel density in the scar area for these three different groups. Determination of blood vessel density 33 days post-implantation. Quantification of α-SMA-stained vessels. $^{***}P \leqslant 0.001$, based on ANOVA analysis.

important when scaffolds were seeded with MSCs (Fig. 8F, $P > 0.05$).

Interestingly, we observed, in parallel to a tendency for a decrease in ventricular fibrosis, a significant increase in SMA staining (Fig. 9), with a circular morphology typical of vascular walls. Quantification of such SMA staining showed a significant increase in the rat group implanted with acellular scaffolds as compared to rats without implanted scaffolds ($P < 0{,}001$, MI group). The presence of MSCs further increased SMA staining as compared to the acellular scaffold-implanted group ($P < 0.001$). These results suggest that MSCs included in 3D PEC scaffolds promote myocardial angiogenesis.

## 4. Discussion

The aim of this study was to evaluate the potential of MSCs/3D PEC scaffolds for heart tissue engineering. With this in mind, alginate was associated with chitosan, which appears particularly interesting because of its strong mechanical properties and its ability to promote cell adhesion [29]. Opposite-charge PECs generated, after freeze-drying, mixed alginate/chitosan 3D PEC scaffolds. These scaffolds were designed with a patch shape for application onto the myocardium ischemic area. This study reports for the first time the use of chemically unmodified chitosan to improve alginate properties and the design of 3D PEC scaffolds seeded with MSCs for heart tissue engineering. The association of calcium-cross-linked alginate with chitosan resulted in biomimetic and biocompatible scaffolds with adapted microstructure and mechanical properties. In addition, alginate/chitosan scaffolds showed improved in vitro and in vivo performance.

As reported previously by other teams, cardiac tissue is a non-Hookean material with a differential elastic modulus close to 20 kPa [30–33]. All 3D PEC scaffolds displayed mechanical properties with viscoelastic and/or plastic behavior and a differential elastic modulus (between 10 and 40 kPa) compatible with cardiac tissue. Chitosan addition significantly improved the scaffolds' mechanical resistance, which appeared 10–20 times higher than that in pure alginate or pure chitosan scaffolds. Synergistic polymer interaction led to an improvement in the mechanical behavior of 3D PEC scaffolds [27].

After freeze-drying, PEC networks for all alginate/chitosan ratios showed a highly porous interconnected homogeneous structure on surface and cross-sections. Pore dimensions of 50–250 μm, on both surface and cross-sections, were compatible with cell culture. Moreover, MSCs seeded on the surface of 3D PEC scaffolds could be disseminated through the scaffold body by centrifugation. This method appears particularly convenient for 3D cell seeding [18]. In this configuration, cells can be 3D cultured in conditions mimicking the in vivo environment [34–37]. In contrast to alginate, chitosan is well known to improve cell adhesion [29,38] but little is known about the effects of the association of chitosan and alginate on cell adhesion, survival and activities. Our results show that 14 days after seeding, cell metabolic activity in all matrices increased, suggesting that all the PEC scaffolds and combinations of alginate and chitosan stimulate cell proliferation/metabolic activity.

MSC functionality was analyzed 24 h after seeding by quantification of cytokine released in the medium. These results clearly show that polyelectrolyte alginate/chitosan scaffolds increased the ability of MSCs to secrete HGF and FGF-2 as compared to MSC 2D cultures on tissue culture plates. The mechanisms responsible for the changes in paracrine activity of MSCs in scaffolds are unclear. It is possible that interaction of MSCs with biomatrices may activate plasma membrane receptors and/or adhesion proteins regulating the secretory properties of MSCs. Spatial cell configuration, cell density, and the mechanical and chemical properties of 3D scaffolds may also affect paracrine activity [39–43]. Additional studies will be necessary to confirm this hypothesis.

Our objective was to improve the microenvironment of grafted cells in cardiac cell therapy. PEC formation between alginate and

chitosan achieved this goal in terms of scaffold porosity and mechanical properties. Moreover, these scaffolds appeared to have bioactive effects on the cell adhesion and secretory properties.

The evaluation of 3D PEC scaffolds in an acute MI model demonstrated the suitability of these scaffolds for cardiac cell therapy using MSCs. Indeed, the use of MSC/3D PEC scaffolds significantly improved cardiac function, decreased ventricular fibrosis and promoted angiogenesis near the necrotic zone. Some studies previously reported that implantation of acellular biomaterials improved cardiac function. In these acellular strategies, the beneficial effects were related to the mechanical stress exerted by the scaffold on the left ventricle and its ability to overcome the loss of cardiac contractility [44] and mimic extracellular matrix functions [45,46]. Moreover, such devices seemed to prevent ventricular dilatation [47–50]. In our study, we also observed that acellular scaffolds prevented ventricular dilatation after MI. However, ventricular function significantly improved only when implanted 3D PEC scaffolds contained MSCs. The beneficial effects of implanted MSC/3D PEC scaffolds were probably related to the secretion of paracrine factors by MSCs. Indeed, in vitro studies showed that MSCs maintained their ability to secrete HGF, FGF-2 and VEGF when cultured in 3D PEC scaffolds. These growth factors are well known to be involved in the positive effects of MSCs on tissue regeneration after ischemic insult. Indeed, HGF reduces fibrotic response and promotes cytoprotection and angiogenesis [51–54]. FGF-2 and VEGF are also widely reported to be involved in blood vessel formation [55–58]. According to these in vitro results, 3D PEC scaffolds seeded with MSCs improved neovascularization around the necrotic zone after implantation. Interestingly, we found that acellular scaffolds also stimulated angiogenesis, albeit to a lesser extent. Therefore, the increase in angiogenesis after scaffold deposition seems to be related to both the properties of 3D PEC scaffolds and the paracrine activity of MSCs. Other biomimetic materials, composed with fibrinogen, are able to promote cell adhesion and play an important role in angiogenesis [59,60]. 3D PEC scaffolds synthesized with alginate and chitosan have been previously proposed for cartilage and bone tissue engineering [24, 61–64]. As compared to the experimental protocols used in our study, those described for cartilage and bone tissue engineering included generation of hydrated PEC scaffolds without a freeze-drying step, with 50/50 formulation and 4.8% (w/w) of final polymer concentration. This protocol resulted in mechanical properties similar to those of bone tissue (8.16 MPa). Such properties significantly differ from those of heart tissue and our 3D PECs. It has also been shown that 3D PEC scaffolds can support MSC culture for 14 days, and the biocompatibility of the construct after implantation in rats has been demonstrated.

Our work reports for the first time the combination of alginate and chitosan to generate highly porous scaffolds answering to specifications required for both 3D culture and cardiac implantation. Our results on cardiac function and tissue cardiac morphology demonstrate the efficacy of this bioengineering approach for cell therapy of ischemic heart disease.

## 5. Conclusions

The present study describes the elaboration and the evaluation of macroporous 3D PEC scaffolds designed to improve alginate scaffold performance in cardiac stem cell therapy. Among the different compositions we tested, the 40/60 alginate/chitosan PEC scaffolds presented a suitable porous microstructure, as well as suitable mechanical and biological properties for in vitro MSC culture. Moreover, after evaluation in a rat model of acute MI, the grafted MSCs enhanced the positive effect of the scaffolds and significantly improved cardiac function. Our results show that these 40/60 3D PEC scaffolds have potential to serve as a useful tool for cardiac tissue engineering.


## Acknowledgements

We are grateful for the excellent technical support and advice of B. Payré and R. d'Angelo (Cellular Imaging Facility, IFR150-Rangueil, TRI Plateform, Toulouse). We thank S. Estage and A. Estival for assistance with tissue embedding and processing (Service d'anatomie et cytology pathologiques, CHU Rangueil, Toulouse). This work was supported by CNRS (CNRS grant for exploratory projects "Interface Matériau/Vivant").


## Appendix A. Figures with essential colour discrimination

Certain figures in this article, particularly Figs. 2, 3 and 6–9 are difficult to interpret in black and white. The full colour images can be found in the on-line version, at http://dx.doi.org/10.1016/j.actbio.2013.10.027.

## References


[1] Shah RV, Holmes D, Anderson M, Wang TY, Kontos MC, Wiviott SD, et al. Risk of heart failure complication during hospitalization for acute myocardial infarction in a contemporary population: insights from the national cardiovascular data ACTION registry. Circ Heart Fail 2012;5(6):693–702.

[2] Segers VF, Lee RT. Stem-cell therapy for cardiac disease. Nature 2008;451(7181):937–42.

[3] Galvez-Monton C, Prat-Vidal C, Roura S, Soler-Botija C, Bayes-Genis A. Cardiac tissue engineering and the bioartificial heart. Rev Esp Cardiol 2013;66(5):391–9.

[4] Caplan AI. Adult mesenchymal stem cells for tissue engineering versus regenerative medicine. J Cell Physiol 2007;213(2):341–7.

[5] Caplan AI, Dennis JE. Mesenchymal stem cells as trophic mediators. J Cell Biochem 2006;98(5):1076–84.

[6] Tang J, Xie Q, Pan G, Wang J, Wang M. Mesenchymal stem cells participate in angiogenesis and improve heart function in rat model of myocardial ischemia with reperfusion. Eur J Cardiothorac Surg 2006;30(2):353–61.

[7] Yagi H, Soto-Gutierrez A, Parekkadan B, Kitagawa Y, Tompkins RG, Kobayashi N, et al. Mesenchymal stem cells: mechanisms of immunomodulation and homing. Cell Transplant 2010;19(6):667–79.

[8] Roncalli J, Mouquet F, Piot C, Trochu JN, Le Corvoisier P, Neuder Y, et al. Intracoronary autologous mononucleated bone marrow cell infusion for acute myocardial infarction: results of the randomized multicenter BONAMI trial. Eur Heart J 2011;32(14):1748–57.

[9] Maurel A, Azarnoush K, Sabbah L, Vignier N, Le Lorc'h M, Mandet C, et al. Can cold or heat shock improve skeletal myoblast engraftment in infarcted myocardium? Transplantation 2005;80(5):660–5.

[10] Muller-Ehmsen J, Whittaker P, Kloner RA, Dow JS, Sakoda T, Long TI, et al. Survival and development of neonatal rat cardiomyocytes transplanted into adult myocardium. J Mol Cell Cardiol 2002;34(2):107–16.

[11] Reinecke H, Zhang M, Bartosek T, Murry CE. Survival, integration, and differentiation of cardiomyocyte grafts: a study in normal and injured rat hearts. Circulation 1999;100(2):193–202.

[12] Tambara K, Sakakibara Y, Sakaguchi G, Lu F, Premaratne GU, Lin X, et al. Transplanted skeletal myoblasts can fully replace the infarcted myocardium when they survive in the host in large numbers. Circulation 2003;108(Suppl. 1):II259–63.

[13] Toma C, Pittenger MF, Cahill KS, Byrne BJ, Kessler PD. Human mesenchymal stem cells differentiate to a cardiomyocyte phenotype in the adult murine heart. Circulation 2002;105(1):93–8.

[14] Westrich J, Yaeger P, He C, Stewart J, Chen R, Seleznik G, et al. Factors affecting residence time of mesenchymal stromal cells (MSC) injected into the myocardium. Cell Transplant 2010;19(8):937–48.

[15] Chandy T, Rao GH, Wilson RF, Das GS. The development of porous alginate/elastin/PEG composite matrix for cardiovascular engineering. J Biomater Appl 2003;17(4):287–301.

[16] Hyun JS, Tran MC, Wong VW, Chung MT, Lo DD, Montoro DT, et al. Enhancing stem cell survival in vivo for tissue repair. Biotechnol Adv 2013;31(5):736–43.

[17] Grant GT, Morris ER, Rees DA, Smith PJC, Thom D. Biological interactions between polysaccharides and divalent cations: the egg-box model. FEBS Lett 1973;32(1):195–8.

[18] Dar A, Shachar M, Leor J, Cohen S. Optimization of cardiac cell seeding and distribution in 3D porous alginate scaffolds. Biotechnol Bioeng 2002;80(3):305–12.

[19] Dvir T, Benishti N, Shachar M, Cohen S. A novel perfusion bioreactor providing a homogenous milieu for tissue regeneration. Tissue Eng 2006;12(10):2843–52.

[20] Leor J, Aboulafia-Etzion S, Dar A, Shapiro L, Barbash IM, Battler A, et al. Bioengineered cardiac grafts: a new approach to repair the infarcted myocardium? Circulation 2000;102(19 Suppl. 3):III56–61.

[21] Schwarzkopf R, Shachar M, Dvir T, Dayan Y, Holbova R, Leor J, et al. Autospecies and post-myocardial infarction sera enhance the viability, proliferation, and maturation of 3D cardiac cell culture. Tissue Eng 2006;12(12):3467–75.
[22] Leor J, Gerecht S, Cohen S, Miller L, Holbova R, Ziskind A, et al. Human embryonic stem cell transplantation to repair the infarcted myocardium. Heart 2007;93(10):1278–84.
[23] Ceccaldi C, Fullana SG, Alfarano C, Lairez O, Calise D, Daniel C, et al. Alginate scaffolds for mesenchymal stem cell cardiac therapy: influence of alginate composition. Cell Transplant 2012;21(9):1969–84.
[24] Wang H, Zhang X, Li Y, Ma Y, Zhang Y, Liu Z, et al. Improved myocardial performance in infarcted rat heart by co-injection of basic fibroblast growth factor with temperature-responsive chitosan hydrogel. J Heart Lung Transplant 2010;29(8):881–7.
[25] Howling GI, Dettmar PW, Goddard PA, Hampson FC, Dornish M, Wood EJ. The effect of chitin and chitosan on fibroblast-populated collagen lattice contraction. Biotechnol Appl Biochem 2002;36(Pt 3):247–53.
[26] Altman AM, Gupta V, Rios CN, Alt EU, Mathur AB. Adhesion, migration and mechanics of human adipose-tissue-derived stem cells on silk fibroin-chitosan matrix. Acta Biomater 2010;6(4):1388–97.
[27] Li Z, Ramay HR, Hauch KD, Xiao D, Zhang M. Chitosan-alginate hybrid scaffolds for bone tissue engineering. Biomaterials 2005;26(18):3919–28.
[28] Shapiro L, Cohen S. Novel alginate sponges for cell culture and transplantation. Biomaterials 1997;18(8):583–90.
[29] Howling GI, Dettmar PW, Goddard PA, Hampson FC, Dornish M, Wood EJ. The effect of chitin and chitosan on the proliferation of human skin fibroblasts and keratinocytes in vitro. Biomaterials 2001;22(22):2959–66.
[30] Cheng AY, Garcia AJ. Engineering the matrix microenvironment for cell delivery and engraftment for tissue repair. Curr Opin Biotechnol 2013;24(5):864–71.
[31] Holzapfel BM, Reichert JC, Schantz JT, Gbureck U, Rackwitz L, Noth U, et al. How smart do biomaterials need to be? A translational science and clinical point of view. Adv Drug Deliv Rev 2013;65(4):581–603.
[32] Vogt M, Jacob R. Myocardial elasticity and left ventricular distensibility as related to oxygen deficiency and right ventricular filling. Analysis in a rat heart model. Basic Res Cardiol 1985;80(5):537–47.
[33] Berry MF, Engler AJ, Woo YJ, Pirolli TJ, Bish LT, Jayasankar V, et al. Mesenchymal stem cell injection after myocardial infarction improves myocardial compliance. Am J Physiol Heart Circ Physiol 2006;290(6):H2196–203.
[34] Cukierman E, Pankov R, Stevens DR, Yamada KM. Taking cell-matrix adhesions to the third dimension. Science 2001;294(5547):1708–12.
[35] Cukierman E, Pankov R, Yamada KM. Cell interactions with three-dimensional matrices. Curr Opin Cell Biol 2002;14(5):633–9.
[36] Gerecht S, Townsend SA, Pressler H, Zhu H, Nijst CL, Bruggeman JP, et al. A porous photocurable elastomer for cell encapsulation and culture. Biomaterials 2007;28(32):4826–35.
[37] Hsiong SX, Huebsch N, Fischbach C, Kong HJ, Mooney DJ. Integrin-adhesion ligand bond formation of preosteoblasts and stem cells in three-dimensional RGD presenting matrices. Biomacromolecules 2008;9(7):1843–51.
[38] Rowley JA, Madlambayan G, Mooney DJ. Alginate hydrogels as synthetic extracellular matrix materials. Biomaterials 1999;20(1):45–53.
[39] Dado D, Levenberg S. Cell-scaffold mechanical interplay within engineered tissue. Semin Cell Dev Biol 2009;20(6):656–64.
[40] Stabler C, Wilks K, Sambanis A, Constantinidis I. The effects of alginate composition on encapsulated betaTC3 cells. Biomaterials 2001;22(11):1301–10.
[41] Engler AJ, Sen S, Sweeney HL, Discher DE. Matrix elasticity directs stem cell lineage specification. Cell 2006;126(4):677–89.
[42] Kloxin AM, Kloxin CJ, Bowman CN, Anseth KS. Mechanical properties of cellularly responsive hydrogels and their experimental determination. Adv Mater 2010;22(31):3484–94.
[43] Weir MD, Xu HH. Human bone marrow stem cell-encapsulating calcium phosphate scaffolds for bone repair. Acta Biomater 2010;6(10):4118–26.
[44] Yu J, Gu Y, Du KT, Mihardja S, Sievers RE, Lee RJ. The effect of injected RGD modified alginate on angiogenesis and left ventricular function in a chronic rat infarct model. Biomaterials 2009;30(5):751–6.
[45] Landa N, Miller L, Feinberg MS, Holbova R, Shachar M, Freeman I, et al. Effect of injectable alginate implant on cardiac remodeling and function after recent and old infarcts in rat. Circulation 2008;117(11):1388–96.
[46] Shuman JA, Zurcher JR, Sapp AA, Burdick JA, Gorman 3rd RC, Gorman JH, et al. Localized targeting of biomaterials following myocardial infarction: a foundation to build on. Trends Cardiovasc Med 2013.
[47] Davis ME, Hsieh PC, Grodzinsky AJ, Lee RT. Custom design of the cardiac microenvironment with biomaterials. Circ. Res. 2005;97(1):8–15.
[48] Christman KL, Lee RJ. Biomaterials for the treatment of myocardial infarction. J Am Coll Cardiol 2006;48(5):907–13.
[49] Leor J, Landa N, Cohen S. Renovation of the injured heart with myocardial tissue engineering. Exp Rev Cardiovasc Ther 2006;4(2):239–52.
[50] Wall ST, Walker JC, Healy KE, Ratcliffe MB, Guccione JM. Theoretical impact of the injection of material into the myocardium: a finite element model simulation. Circulation 2006;114(24):2627–35.
[51] Esposito C, Parilla B, De Mauri A, Cornacchia F, Fasoli G, Foschi A, et al. Hepatocyte growth factor (HGF) reduces the expression of profibrotic factors in human isolated glomeruli. G Ital Nefrol 2003;20(4):376–80.
[52] Tomita N, Morishita R, Taniyama Y, Koike H, Aoki M, Shimizu H, et al. Angiogenic property of hepatocyte growth factor is dependent on upregulation of essential transcription factor for angiogenesis, ets-1. Circulation 2003;107(10):1411–7.
[53] Wang Y, Ahmad N, Wani MA, Ashraf M. Hepatocyte growth factor prevents ventricular remodeling and dysfunction in mice via Akt pathway and angiogenesis. J Mol Cell Cardiol 2004;37(5):1041–52.
[54] Jayasankar V, Woo YJ, Pirolli TJ, Bish LT, Berry MF, Burdick J, et al. Induction of angiogenesis and inhibition of apoptosis by hepatocyte growth factor effectively treats postischemic heart failure. J Card Surg 2005;20(1):93–101.
[55] Simons M. Integrative signaling in angiogenesis. Mol Cell Biochem 2004;264(1–2):99–102.
[56] Presta M, Dell'Era P, Mitola S, Moroni E, Ronca R, Rusnati M. Fibroblast growth factor/fibroblast growth factor receptor system in angiogenesis. Cytokine Growth Factor Rev 2005;16(2):159–78.
[57] Vandervelde S, van Luyn MJ, Tio RA, Harmsen MC. Signaling factors in stem cell-mediated repair of infarcted myocardium. J Mol Cell Cardiol 2005;39(2):363–76.
[58] Kim SH, Moon HH, Kim HA, Hwang KC, Lee M, Choi D. Hypoxia-inducible vascular endothelial growth factor-engineered mesenchymal stem cells prevent myocardial ischemic injury. Mol Ther 2011;19(4):741–50.
[59] Westlin WF. Integrins as targets of angiogenesis inhibition. Cancer J 2001;7(Suppl. 3):S139–43.
[60] Haubner R. Alphavbeta3-integrin imaging: a new approach to characterise angiogenesis? Eur J Nucl Med Mol Imaging 2006;33(Suppl. 1):54–63.
[61] Li Z, Zhang M. Chitosan-alginate as scaffolding material for cartilage tissue engineering. J Biomed Mater Res A 2005;75(2):485–93.
[62] Li X, Yu X, Lin Q, Deng C, Shan Z, Yang M, et al. Bone marrow mesenchymal stem cells differentiate into functional cardiac phenotypes by cardiac microenvironment. J Mol Cell Cardiol 2007;42(2):295–303.
[63] Florczyk SJ, Kim DJ, Wood DL, Zhang M. Influence of processing parameters on pore structure of 3D porous chitosan-alginate polyelectrolyte complex scaffolds. J Biomed Mater Res A 2011;15(4):614–20.
[64] Florczyk SJ, Leung M, Li Z, Huang JI, Hopper RA, Zhang M. Evaluation of three-dimensional porous chitosan-alginate scaffolds in rat calvarial defects for bone regeneration applications. J Biomed Mater Res A 2013;101(10):2974–83.